

# Low-Cost Channel Sounder design based on Software-Defined Radio and OFDM

Yasser Samayoa\*, Markus Kock†, Holger Blume†, Jörn Ostermann\*

\**Institut für Informationsverarbeitung*, †*Institut für Mikroelektronische Systeme*,

*Gottfried Wilhelm Leibniz Universität Hannover*

30167 Hanover, Germany

Email: \*{samayoa, office}@tnt.uni-hannover.de, †{kock, blume}@ims.uni-hannover.de

**Abstract**—In this paper we describe the design of a low-cost and portable channel sounding system. The baseband signal processing in both the transmitter and the receiver are done in software, while the up/down conversion are done by means of a Software Defined Radio (SDR) frontend. The modulation procedure is based on the Orthogonal Frequency Division Multiplexing (OFDM) technique due to its robustness against inter-symbol interference (ISI). The sounder is designed to overcome some well known important issues of any OFDM system. For example, it does not need extra resources neither to guarantee a ISI-free transmission by means of a guard interval, nor for the synchronization by means of a preamble. Moreover, the excitation signal is designed to have a peak-to-average power ratio (PAPR) close to 0 dB while maintaining a flat spectrum. The system is calibrated and validated under laboratory conditions prior to the measurement of an air-to-ground channel in the C frequency band, the results are presented and discussed.

**Index Terms**—Channel sounding, channel estimation, OFDM, PAPR, multitone, power-delay spectrum, Doppler-delay spectrum

## I. INTRODUCTION

Good performance at a high data rate has become a constant growing prerequisite for deploying communication systems. This places new challenges that require suitable channel models in order to optimize the systems designs. Nevertheless, due to its complicated nature, detailed analysis and models are not always feasible or available, therefore, channel sounding campaigns are a requisite to acquire channel models. Conventional channel sounding campaigns are mostly implemented using commercial equipment with different sounding techniques [1] [2]. Besides their high cost, this equipment is not flexible in terms of mobility.

Orthogonal Frequency Division Multiplexing (OFDM) modulation technology is widely used in communications systems due to its capability in avoiding inter-symbol interference (ISI) by inserting a guard interval (GI) [3]. Nevertheless, some of its drawbacks are its large peak-to-average power ratio (PAPR) and its sensitivity to any deviation on the time-frequency synchronization stage. High PAPR signals demand expensive and inefficient power amplifiers, while synchronization is normally acquired using a preamble. Both preambles and GI reduce thus the OFDM system efficiency in terms of spectrum and energy. Sounders based on the OFDM technology have been used with commercial equipments [4] and with software-defined radios (SDR) as well. The last group

of sounders normally uses a packet-oriented OFDM signal with GI and without an optimized PAPR signal [5]–[9].

In this paper we propose a mobile OFDM-based channel sounder system using low-cost SDR for the up/down conversion. The proposed sounder overcomes the drawback of conventional OFDM systems mentioned above, i.e., the excitation signal is designed with very low PAPR while GI, preamble, and packet-oriented transmission are not required, which improves the spectral efficiency and saves transmission energy in comparison to other OFDM-based sounders.

The remainder of this paper is organized as follows. In Section II, the channel is described mathematically while in Section III the channel sounder is presented. In Section IV a validation of the sounder together with a measurement campaign are detailed. The paper concludes and summarizes its main contribution in Section V.

## II. WIRELESS MOBILE CHANNEL

A widely accepted assumption is that wireless channels are nondeterministic linear systems. For example, an equivalent low-pass channel impulse response (CIR) can be modeled as a sum of a number of time-variant phasors [10], i.e.,

$$h(n, t) = \sum_n \alpha(n, t) e^{-j\theta(n, t)}, \quad (1)$$

where  $\alpha(n; t)$  denotes its attenuation whereas  $\theta(n, t)$  gives its phase, both at delay  $n = 0, 1, 2, \dots, N - 1$  and time instant  $t = 0, 1, 2, \dots, M - 1$ . The sample vector in (1) is the time history record of length  $M$  from a single sample function of the discrete-time, complex-valued and zero-mean Gaussian random process in the  $t$  variable. Thus,  $M$  is the total number of CIR considered in (1) and  $N$  is the length of a single CIR at time  $t$ . A valid assumption is that (1) is wide sense ergodic, therefore, wide sense stationary (WSS) in the  $t$  variable. The time-varying complex transfer function of (1) is then given by an N-point DFT

$$H(k, t) = \sum_n h(n, t) e^{-j2\pi nk/N}, \quad (2)$$

with  $k = 0, 1, 2, \dots, N - 1$ . In order to characterize (1), it is convenient to define the time-frequency autocorrelation function (ACF) of (2) for arbitrary frequencies  $k_1$  and  $k_2$

evaluated at time  $t_1$  and  $t_2$  respectively. This can be expressed as

$$\phi_H(k_1, k_2; t_1, t_2) = \mathbb{E}[H(k_1, t_1)H^*(k_2, t_2)]. \quad (3)$$

where  $(\cdot)^*$  represent the complex conjugate operator. Since the channel is WSS in the  $t$  variable, (3) does not depend on the absolute time values  $t_1$  and  $t_2$ , but on the difference  $\Delta t = t_1 - t_2$ , i.e.,  $\phi_H(f_1, f_2; t_1, t_2) = \phi_H(f_1, f_2; t, t + \Delta t) = \phi_H(f_1, f_2; \Delta t)$  for any time  $t$ . A second assumption is that the channel  $h(n, t)$  has uncorrelated scattering (US), which means that the attenuation and phase shift in (1) due to  $n_1$  is uncorrelated with the attenuation and phase shift due to  $n_2$ . As a result, (3) does not depend on the absolute frequency values  $f_1$  and  $f_2$ , but on the difference  $\Delta k = k_1 - k_2$ , i.e.,  $\phi_H(k_1, k_2; \Delta t) = \phi_H(k, k + \Delta k; \Delta t) = \phi_H(\Delta k; \Delta t)$ . Finally, by considering the last assumptions and substituting (2) in (3), it turns out that

$$\phi_H(\Delta k; \Delta t) = \frac{1}{2} \sum_n \mathbb{E}[h(n, t)h^*(n, t + \Delta t)]e^{-j2\pi\Delta kn/N} \quad (4a)$$

$$= \sum_n \phi_h(n, \Delta t)e^{-j2\pi\Delta kn/N}. \quad (4b)$$

Note that  $\phi_h(n; \Delta t)$  is the average power output of the channel. If we let  $\Delta t = 0$ ,  $\phi_h(n; t)$  results in the average power output of the channel as a function of the time delay  $n$  at time  $t$ .

Now we are able to define the scattering function of the channel denoted by  $S(\lambda, n)$ . This provides a measure of the average power output of the channel as a function of the time delay  $n$  and the Doppler frequency  $\lambda$ . It is defined as follows

$$S(n; \lambda) = \sum_{\Delta k, \Delta t} \phi_H(\Delta k; \Delta t)e^{-j2\pi n\Delta k/N}e^{-j2\pi\lambda\Delta t/N}, \quad (5a)$$

$$= \sum_{\Delta t} \phi_h(n; \Delta t)e^{-j2\pi\lambda\Delta t/N}. \quad (5b)$$

From  $S(n; \lambda)$  the delay power spectrum  $\phi_c(n)$  and the doppler power spectrum  $S_c(\lambda)$  of the channel can be straightforward computed by

$$\phi_c(n) = \sum_{\lambda} S(n; \lambda) \quad \text{and} \quad S_c(\lambda) = \sum_n S(n; \lambda). \quad (6)$$

### III. SOUNDER SYSTEM DESCRIPTION

The block diagram of the proposed channel sounding is depicted in Figure 1. The transmitter PC reads the discrete-time signal  $x(n)$  over  $0 \leq n \leq N - 1$  previously stored in memory and sends it periodically to the SDR<sub>TX</sub> such that

$$\tilde{x}(n) = \sum_{t=0}^{M-1} x(n - tN), \quad (7)$$

where  $x(n)$  is a N-point complex sequence in the discrete-time domain and  $\tilde{x}(n)$  is a periodic signal with period  $N$  so that

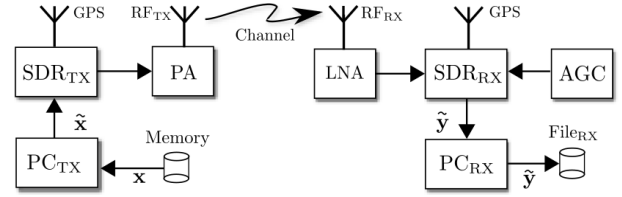


Fig. 1: Channel sounder system block diagram

$\tilde{x}(n) = x(n)$  for  $0 \leq n \leq N - 1$ . The SDR<sub>TX</sub> receives the complex-valued baseband signal and basically up converts it to a real-valued signal prior to its transmission to the air over the antenna. At the receiver, the SDR<sub>RX</sub> down converts the received signal to the discrete-time, complex-valued baseband domain and sends it to the receiver PC<sub>RX</sub> which stores it in a binary file for post processing. The signal processing in both the transmitter and the receiver is accomplished offline.

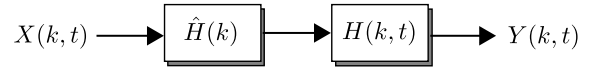


Fig. 2: Signal processing block diagram of the channel sounder in frequency domain

The strategy of the sounder can be viewed in frequency domain as depicted in Figure 2. The transmitter conveys the  $t$ -th symbol  $X(k, t) = \text{DFT}_N\{x(n, t)\}$  to excite the channel. Assuming a perfect synchronization between transmitter and receiver, the output of the channel is

$$Y(k, t) = X(k, t)\hat{H}(k)H(k, t), \quad (8)$$

where  $\hat{H}(k)$  gives the transfer function of the sounding system itself (eg., amplifiers, cables, etc.);  $H(k, t)$  is the channel transfer function to be estimated at time  $t$  corresponding to (2). From (8), the estimation of  $H(k, t)$  is straightforward under the condition that there is neither inter-symbol interference (ISI) nor inter-carrier interference (ICI). It is well known that OFDM systems ensure ISI-free communication through the insertion of guard intervals (GI) in the time domain signal. The length of GI has to be equal to or longer than the overall channel impulse response in order to preserve the orthogonality of the subcarriers [3]. The GI space can be filled with zeros (zero padding) or with the last samples of the signal known as cyclic prefix (CP). This last approach gives the best result and it is therefore the most widely used solution. Following this rationale, the signal given in (7) is equivalent to an OFDM signal with CP, since any symbol sent at  $t - 1$  serves as a CP for the symbol sent at  $t$ . In other words, ISI-free is achieved due to the periodicity of  $\tilde{x}(n)$  under the condition that the length of the CIR does not exceed the length of  $x(n)$ . On the other hand, ICI-free is accomplished by the synchronization procedure on the receiver side which takes advantage of the periodicity of  $\tilde{y}(n)$  without requiring a preamble.

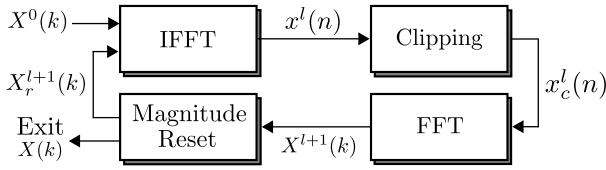


Fig. 3: Crest factor reduction algorithm

#### A. Signal Processing at the Sounder Transmitter

We find that any DFT pair  $x(n)$  and  $X(k)$  can be selected to excite the channel as long as it meets the following requirements:

- R.1 A constant spectrum of  $X(k)$ . This ensures equal power transmission over its bandwidth.
- R.2 Small PAPR of  $x(n)$ . This allows an efficient use of the power amplifier.
- R.3 Low side-lobes in the ACF of  $x(n)$  to help the synchronization stage at the receiver.
- R.4  $N$  must be longer than the length of the CIR.

The procedure proposed in [11] is employed here to obtain a suitable signal  $X(k)$ . The main idea is to swap between the time and frequency domain imposing some constraints on the signal on either domain. Figure 3 presents the algorithm. We begin by defining  $N$  and a constant crest factor  $A_{CF}$  equal to the root mean square (RMS) of the time signal as the maximum peak allowed in the time signal  $x(n)$ . The algorithm begins by initializing

$$X^l(k) = [A_k^l e^{j\phi_k^l}]_{k=0}^{N-1}, \quad \text{for } l = 0, \quad (9)$$

where  $A_k^l \in \mathbb{R}$ , and  $\phi_k^l \in [0, 2\pi)$  are selected arbitrarily,  $l$  denotes the iteration index. For our purpose  $A_k^l = 1$  for all  $k, l$ ; and  $\phi_k^l$  is chosen randomly for all  $k$  and  $l = 0$ . The signal in (9) is transformed to the time domain  $x^l(n) = \text{IFFT}_N\{X^l(k)\} = [A_n^l e^{j\phi_n^l}]_{n=0}^{N-1}$  and then clipped to the predetermined value  $A_{CF} = \text{RMS}\{X^0(k)\}$ , i.e.,

$$x_c^l(n) = \begin{cases} A_n^l e^{j\phi_n^l} & \text{if } |A_n^l| \leq A_{CF} \\ A_{CF} e^{j\phi_n^l} & \text{if } |A_n^l| > A_{CF} \end{cases}, \quad \forall n.$$

The clipped version  $x_c^l(n)$  is then transformed to the frequency domain  $X^{l+1}(k) = \text{FFT}_N\{x_c^l(n)\} = [A_k^{l+1} e^{j\phi_k^{l+1}}]_{k=0}^{N-1}$  and its magnitude is reset to 1, i.e.,  $X_r^{l+1}(k) = e^{j\phi_k^{l+1}}$  for all  $k$ . Note that only the magnitudes are modified in both frequency and time domain, the phases are modified through the clipping operation. The algorithm continues until some criteria is fulfilled, e.g., the CF has converged or until a prior defined maximum number of iterations has been reached.

#### B. Signal Processing at the Sounder Receiver

Figure 4 introduces the strategy employed for the signal post-processing. Each block is introduced in the following sections.

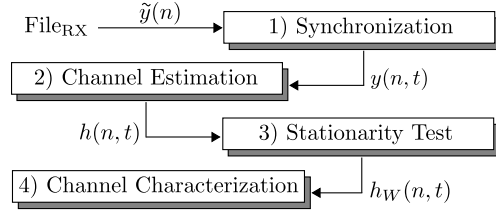


Fig. 4: Data post-processing at the sounder receiver

1) *Synchronization*: As it is usual for OFDM symbols, in the proposed sounding system time and frequency synchronizations are also required. Explicitly, symbol time offset (STO) synchronization and a carrier frequency offset (CFO) correction must be performed for each symbol.

The goal of the STO synchronization is to identify the precise moment of when individual symbols starts. This can be accomplished by cross-correlating the reference sequence  $x(n)$  with the received sequence  $\tilde{y}(n)$  of period  $N$ . The output of the correlation function is periodic with peaks  $N/2$  apart from the exact start position of each symbol. The ACF property of  $x(n)$  is thus exploited. The output of the STO synchronization is then  $\hat{y}(n, t)$ ,  $0 \leq t \leq M - 1$  which has the exact position of each symbol and  $0 \leq n \leq N - 1$  gives its length.

The CFO must be corrected to preserve the orthogonality of the OFDM subcarriers i.e., avoiding thus ICI. The CFO is found and corrected for each OFDM symbol received  $y(n, t)$ , following [12]. We estimate it in time domain by means of

$$f_{\text{cfo}}(t) = \sum_{n=0}^{N-1} \left\{ \frac{\angle[\hat{y}(n, t)\hat{y}^*(n, t+1)]}{2\pi N^2} \right\}. \quad (10)$$

Note that CFO in (10) is normalized by the sampling frequency  $f_s$  and that a  $f_{\text{cfo}}(t)$  for each received OFDM symbol is found. Finally, the CFO correction is performed as follows

$$y(n, t) = \hat{y}(n, t)e^{-j2\pi f_{\text{cfo}}(t)}, \quad \forall n, t. \quad (11)$$

At this stage, a time-frequency synchronized vector has been reached without any preamble.

2) *Channel Estimation*: The channel estimation is performed independently for each  $t$ -th symbol in frequency domain, from (8) this leads to

$$H(k, t) = \frac{\text{FFT}_N\{y(n, t)\}}{X(k)\hat{H}(k)}, \quad \forall k, t, \quad (12)$$

where  $X(k)$  is the reference sequence found in Section III-A and  $\hat{H}(k)$  is found in the back-to-back test in section IV-A. The corresponding channel impulse response is defined as

$$h(n, t) = \text{IFFT}_N\{H(k, t)\}, \quad \text{wrt. } k, \forall t. \quad (13)$$

The vector given in (13) is a realization of a discrete-time, complex random process  $\{h(n, t)\}$  introduced in (1). It can be considered as vector of length  $M$  in which each element is a snapshot of the channel at time  $t$ .

3) *Stationarity Test*: The scattering function of the channel can be computed from the previously estimated channels if the WSS condition is true. To test for WSS a statistical test called the RUN test [13] can be applied [2] to the time series data  $\sigma(t)$ , where  $\sigma(t)$  is the root mean square (RMS) value of (13) for all  $t$ . As a result of this stage, the CIRs in (13) are divided in smaller sections or windows denoted by  $W$ , each one collecting consecutive CIRs where the WSS assumption is more likely to hold.

4) *Channel Characterization*: The channel is characterized for a given time window  $W$  in which the channel is assumed WSS. The characterization is done in terms of its delay power spectrum  $\phi_{c,W}(n)$  and Doppler power spectrum  $S_{c,W}(\lambda)$  given in (6). To this end, we first have to compute the scattering function of the channel  $S_W(n; \lambda)$  following (5) over  $0 \leq n \leq N - 1$  and  $0 \leq t \leq w$ , where  $w$  is the length of the window  $W$ .

5) *Practical Comments*: Prior to any measurement, the sounder system has to be dimensioned under some assumptions. Firstly, the length of the excitation signal  $N$  should be larger than the maximum delay of the channel. Secondly,  $N$  should be shorter than the coherence time of the channel which is inversely proportional to the Doppler bandwidth. If these assumptions do not hold, the channel can not be estimated. Therefore, these parameters have to be estimated during a pre channel measurement, in which excitations signals with different length should be tested.

Care should be taken regarding the gain of the receiver adjusted by the auto gain control (AGC). Estimated channels recorded with different gain configuration should be properly weighted. Therefore, the receivers store AGC values and GPS-based absolute timestamps along with the down-converted received signal stream  $\tilde{y}(n)$  while the transmitter logs its flight trajectory.

## IV. CHANNEL SOUNDING CAMPAIGN AND RESULT

### A. Initial Calibration

Prior to the measurement campaigns, the transmitter and the receiver are calibrated in laboratory conditions. The antennas are eliminated and the transmitter is connected to the receiver with a cable, simulating thus a constant channel transfer function. Therefore, in this back-to-back test the calibration of the local oscillators (LO) is verified and the channel  $\hat{H}(k)$  required by (12) is estimated.

The verification of the LO consists of transmitting an unmodulated carrier and measuring its Doppler power spectrum. The maximum and the minimum Doppler power spectrum should be symmetric with respect to  $\lambda = 0$  and the Doppler bandwidth should tend to 0, which is achieved by means of an external GPS-disciplined, oven-controlled crystal oscillator (GPSDO). This ensures the stability and the frequency accuracy to less than one parts per billion (ppb) [14]. The calibration is corroborated by means of a spectrum analyzer and the sounder is validated with a two-path channel made of cables with different lengths and joined with splitters.

TABLE I: Measurement Parameters

Parameter	Value
Measurement bandwidth	20 MHz
Carrier frequency	5.190 GHz
DFT size $N$	512
Symbol duration	25.6 $\mu$ s
SDR platform	Ettus B210
Antenna TX	dipole
Antenna RX	dipole
Channel impulse response resolution	50 ns
Transfer function frequency resolution	39.06 kHz
Measurement time	2 Hrs
Transmitted power	3 W

### B. Sounding Campaign

The sounding system was employed to measure the air-to-ground channel in the city of Hanover, Germany. The transmitter was installed in a helicopter, and three receivers were placed on the ground. Batteries were used for the power supply of the sounder and receivers. Receiver-A was installed on the parking court at the University; Receiver-B was installed on the roof of a building approximately 70 meters above the ground; and Receiver-C was placed at an arbitrary place in the city. The two hours flight route was established to follow three patterns, namely, circles around the receivers, circles far from the receivers without including them and figure of eights. These patterns were chosen to cover a wide range of representative channel realizations commonly found in real flights. The multi-dimensional physical channel impulse response for a 20 MHz wide channel is sampled in time and frequency with a resolution of 50 ns and 39.06 kHz respectively, resulting from the sampling frequency and DFT size. Table I summarizes important system parameters of the sounding campaign.

### C. Measurement Results

In this section, the results and characterization of four channels according to the procedure described in Section III-B for a proof of concept are presented. The channels are measured within a time span of ca. one second by the Receiver-A. Table II and Figure 5 summarize important parameters. As mentioned before, the flight route followed three patterns from which the one depicting a circle around the receiver gives the lowest Doppler shift but the largest Doppler spread. It also gives the shorter windows in which the channel can

TABLE II: Flight parameters of measurements with respect to Receiver-A

Label	Altitude [m]	Distance [m]	Ground speed [km/h]
M-1	496	839	145
M-2	486	738	116
M-3	510	2,229	130
M-4	507	1,958	129

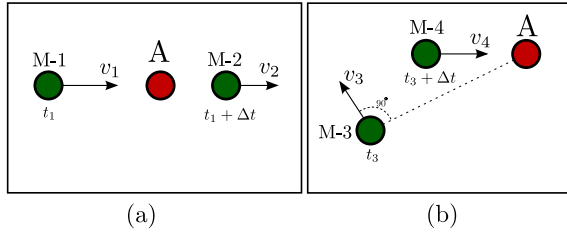


Fig. 5: Illustration of the measurement points  $\{M-i\}_{i=1}^4$  and its velocity vector  $\{v_i\}_{i=1}^4$  with respect to the Receiver-A,  $\Delta t$  is less than 5 seconds.

be considered WSS. The other two patterns present a higher shift but much lower Doppler spread. As an example of these results, Figures 6 and 7 show the channels given in Table II.

A subset of the vector  $h(n, t)$  corresponding to M-1 and its scattering function are plotted in Figure 6. The power delay spectrum and the Doppler power spectrum for all channels are depicted in Figure 7. It can be noticed that the measured Doppler shifts correspond to the theory. For example, given the parameters for M-1 in Table II and Figure 5, the transmitter flies in the direction of the Receiver-A at a velocity of 145 km/h. The channel corresponding to M-1, thus, corresponds to a maximum frequency shift of  $f_{D, \max} = (\text{carrier frequency [Hz]} \cdot \text{speed [m/s]} / \text{speed of light [m/s]}) = 696 \text{ Hz}$  which is the result estimated in Figure 7 as well. Another observation is that the measured Doppler spread of all channels tends to be narrower than the theoretic maximum Doppler bandwidth. This is probably due to the lack of high buildings in the city of Hanover.

The results given by the Receiver-B do not measure any echoes in its CIR but just frequency Doppler shifts because there is no higher structures to produce echoes. The results from the Receiver-C give similar results as from Receiver-A.

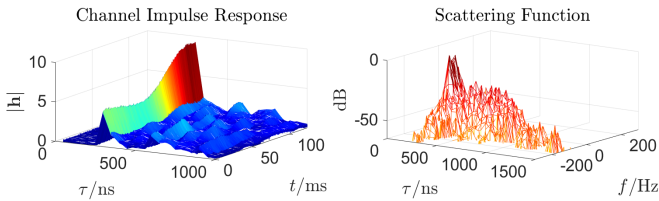


Fig. 6: Illustration of channel impulse responses and the scattering function of the channel corresponding to M-3

## V. CONCLUSION

In this paper we present a low-cost, OFDM-based channel sounder. The up/down conversion is accomplished using a software defined radio (SDR) platform which offers a flexible solution for mobile applications. It is shown that by conveying the excitation signal over the channel periodically, the spectral efficiency is improved when compared with classical OFDM systems, i.e., no guard interval and no preamble are required while ISI-free and ICI-free is guaranteed. Moreover, the excitation signal is designed in such a way that a PAPR close to

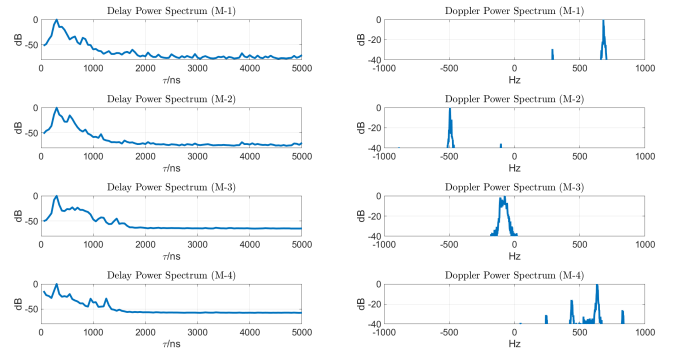


Fig. 7: Delay power spectrum and Doppler power spectrum for  $\{M-i\}_{i=1}^4$

0 dB is achieved for an increased power amplifier efficiency and range. The channel sounder was calibrated and validated successfully in laboratory conditions. Finally, the feasibility of the proposed channel sounder was demonstrated in an air-to-ground channel measurement in the C frequency band in Hanover, Germany.

## REFERENCES

- [1] J. D. Parsons, D. A. Demery, and A. M. D. Turkmani, "Sounding techniques for wideband mobile radio channels: a review," *IEE Proceedings I - Communications, Speech and Vision*, vol. 138, no. 5, pp. 437–446, Oct 1991.
- [2] S. Salous, *Radio Propagation Measurement and Channel Modelling*, John Wiley & Sons, 2013.
- [3] T. Hwang, C. Yang, G. Wu, S. Li, and G. Y. Li, "Ofdm and its wireless applications: A survey," *IEEE Transactions on Vehicular Technology*, vol. 58, no. 4, pp. 1673–1694, May 2009.
- [4] T. Zhou, C. Tao, S. Salous, L. Liu, and Z. Tan, "Implementation of an lte-based channel measurement method for high-speed railway scenarios," *IEEE Transactions on Instrumentation and Measurement*, vol. 65, no. 1, pp. 25–36, Jan 2016.
- [5] H. Boeglen, A. Traore, M. M. Peinado, R. Lefort, and R. Vauzelle, "An sdr based channel sounding technique for embedded systems," *2017 11th European Conference on Antennas and Propagation (EUCAP)*, pp. 3286–3290, March 2017.
- [6] B. Siva Kumar Reddy and B. Lakshmi, "Channel sounding and papr reduction in ofdm for wimax using software defined radio," vol. 2006, no. 11, 2014.
- [7] J. K. Hwang, Kuei-Hong Lin, Yu-Lun Chiu, and Jeng-Da Li, "An ofdm-based multipath channel sounding method with fractional delays resolution," *2010 IEEE International Conference on Wireless Information Technology and Systems*, pp. 1–4, Aug 2010.
- [8] C. Y. Yeh, C. P. Lai, M. C. Tseng, and H. J. Li, "An ofdm-based channel sounder system," *2009 IEEE Antennas and Propagation Society International Symposium*, pp. 1–4, June 2009.
- [9] T. R. Oliveira, W. A. Finamore, and M. V. Ribeiro, "A sounding method based on ofdm modulation for plc channel measurement," *2013 IEEE 17th International Symposium on Power Line Communications and Its Applications*, pp. 185–190, March 2013.
- [10] J. Proakis, *Digital Communications*, McGraw-Hill, 3 edition, 1995.
- [11] M. Friese, "Multitone signals with low crest factor," *IEEE Transactions on Communications*, vol. 45, no. 10, pp. 1338–1344, Oct 1997.
- [12] T. M. Schmidl and D. C. Cox, "Robust frequency and timing synchronization for ofdm," *IEEE Transactions on Communications*, vol. 45, no. 12, pp. 1613–1621, Dec 1997.
- [13] Bendat J.S. and Peirsol, *Measurements and Analysis of Random Data*, John Wiley & Sons, 1996.
- [14] Ettus Research, "Ushr b200/b210 product overview, <https://www.ettus.com/product/details/ub210-kit>," .